Solvation of Ca^{2+} in Water Studied by Born−Oppenheimer ab Initio QM/MM Dynamics

Anan Tongraar, Klaus R. Liedl,* and Bernd M. Rode

Department of Theoretical Chemistry, Institute of General, Inorganic and Theoretical Chemistry, University of Innsbruck, Innrain 52a, A-6020 Innsbruck, Austria

Received: March 18, 1997; In Final Form: June 2, 1997[⊗]

Molecular dynamics simulations based on combined ab initio molecular quantum mechanics and molecular mechanical potentials are applied to investigate the structural and dynamical properties of calcium ion solvated in liquid water. The region of highest interest, the hydration sphere of the calcium ion, is investigated by Born−Oppenheimer ab initio quantum mechanics, while the rest of the system is described by classical pair potentials. A coordination number of 8.3 is found by this high-level QM/MM method with a double-ζ basis set, in contrast to 9.2 obtained by classical pair potential simulations. Dynamical properties are related to the solvate structure. Smaller basis sets have been used to study the influence of basis sets used in the quantum mechanical part.

1. Introduction

Due to the key role calcium ions play in many biological reactions, for example, in signal transduction as in blood clotting and in the transmissions of nerve impulses,[1,2] there is great interest in understanding the solvation of this important ion in every detail. Nevertheless, numerous reports in the literature, both theoretical and experimental,[3−13] provide a rather inhomogeneous picture, even for such fundamental properties as the average number of coordinating solvent molecules.

Calcium ions in crystal structures[13] generally tend to prefer binding to oxygen atoms in ligands rather than to any other element, and their preferred coordination numbers range from 6 to 8. For a solution of Ca^{2+} in water, X-ray diffraction experiments[10] of a 1.0 M $CaCl_2$ solution led to a hydration number of 6, whereas neutron diffraction[9] yielded a value of 10, a rather unexpectedly[12] high value. Coordination numbers of 9.3, 9.2, 8.0, and 7.9 were found by means of molecular dynamics simulations.[3,4,6,7] These simulations relied on classical force fields, in which the potential functions describing the inter- and intramolecular interactions are constructed by fitting an analytical formula to a set of experimental data or to ab initio calculations. Such potentials are usually based on additive pair potentials. It is obvious, however, that the total intermolecular interaction energy for *N*-body systems comprises all of pair, three-body, four-body up to *N*-body interactions:

$$V_{\text{total}} = \sum V(i,j) + \sum V(i,j,k) + ... + \sum V(i,j,k,...,n) \quad (1)$$

The contributions of the higher *N*-body interactions always play a significant role and are even not negligible for rare-gas fluids.[14,15] The effect of nonadditivity in ion−water systems results from the strength of the binding energy between ion and water. For instance, in an aqueous solution of $BeCl_2$,[16] the inclusion of three-body effects for the intermolecular interaction energies causes the hydration number of Be^{2+} to change from 6 to 4, where the latter is the experimental observed coordination number. It has been reported[17,18] that three-body effects for solutions of Ca^{2+} or Mg^{2+} are crucial to obtain reliable hydration numbers and equilibrium distances for the first hydration shell. Although it would be in principle possible to improve potentials by higher order *N*-body terms, one should keep in mind that the construction of potential function including many-body terms becomes hardly tractable for large systems due to the large number of degrees of freedom involved and therefore the high dimensionality.

It has been proposed[19] to compute the potential energy function by an ab initio effective pair potential based on the polarizable continuum model (PCM). This approach includes many-body effects in an average way relying on a continuum polarizable model for the solvent. An average hydration number of 8.6 for Ca^{2+} in water has been found in contrast to 9.1 with pair potentials.[20] However, especially in the first hydration shell of ions, some contributions can be attractive, others might be repulsive, and averaging them is ambiguous and may be misleading. Such averages are responsible for the failure of some effective pair potentials.[21] Complicated nonadditivity effects have also been found for O−H stretching frequency shifts[22] and in nonlinear spectroscopy.[23]

Since fluid systems consisting of a considerable number of molecules are too large to be studied by traditional ab initio calculations directly and the promising Car−Parrinello type simulations are still in an early stage of reliability checking,[24−27] one of the recent approaches is to combine quantum mechanical (QM) and molecular mechanical (MM) methods. Such hybrid approaches have been first published by Warshel and Karplus[28] and by Allinger and Sprague.[29] The methods partition the system into two parts, in which the interaction energy is calculated separately. Most of the early applications of the combined QM/MM method have used only semiempirical treatment for quantum mechanics and usually were restricted to small gas-phase systems.[30−33] In such an approach, however, a strong uncertainty prevails due to the very limited ability of the semiempirical method to describe the geometric and electrostatic properties of the atoms in the quantum mechanical region during the simulation process.[34] The performance of a semiempirical model can vary dramatically according to the selected conditions, and there seems to be no general way to predict a priori how good or bad it will be for the considered case. Nowadays more reliable combined QM/MM methods using high-accuracy molecular quantum mechanics have become available for larger systems, such as condensed phases, due to the availability of fast computers. A detailed description of a QM/MM method to study a condensed-phase system is given by Field et al.[35] A first calculation scheme for the study of ions in solutions by such an approach has been proposed[36] recently and has been applied to Li^+ in liquid ammonia. In

[⊗] Abstract published in *Advance ACS Abstracts,* August 1, 1997.

S1089-5639(97)00963-8 CCC: $14.00

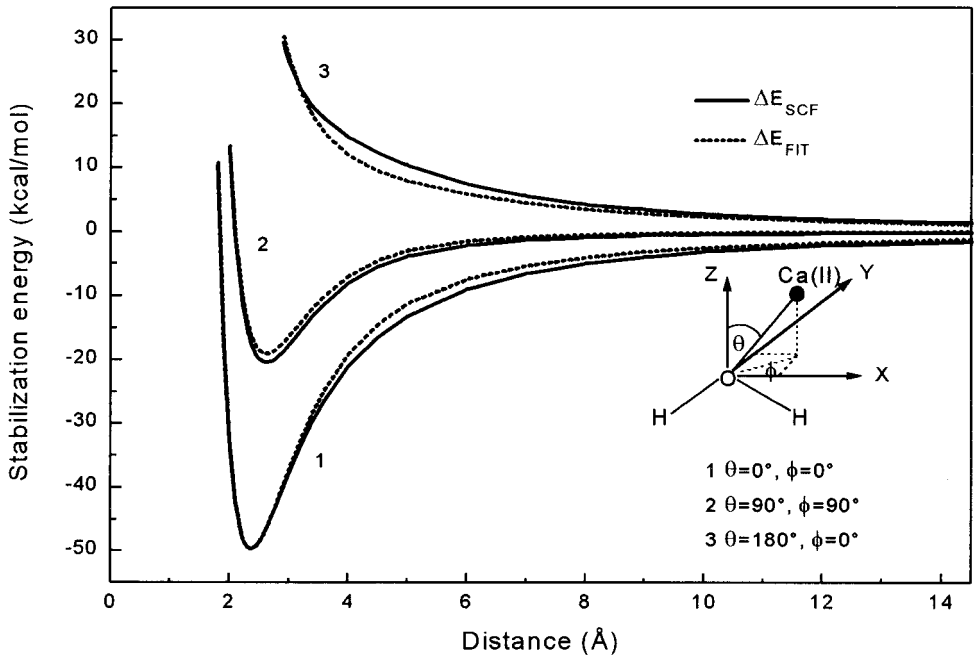

Figure 1. Comparison of the energies obtained from the SCF calculations, ΔE_{SCF} and from the fitted potential function, ΔE_{FIT}, using the parameters given in Table 1 for some values of θ and ϕ.

TABLE 1: Optimized Parameters of the Analytical Pair Potential for the Interaction of O and H Atoms of Water with Calcium Ion (Interaction Energies in kcal mol^{-1} and Distances in Å)

pair	*A* (kcal mol^{-1} Å^6)	*B* (kcal mol^{-1} Å^7)	*C* (kcal mol^{-1})	*D* (Å^{-1})
Ca−O	−21 328.549 69	25 888.989 45	63 073.294 42	3.020 303 01
Ca−H	−6 451.263 420	8 161.930 725	3 262.623 550	2.103 144 04

TABLE 2: Comparison of Solvation Parameters Obtained from Various Methods for Ca^{2+} in Liquid Water (r_{max}, r_{min}, and n_{min} Denote Distance of the First Maximum and the First Minimum in Å, and the Coordination Number of the First Hydration Shell, Respectively)

solute	molarity	r_{max}	r_{min}	n_{min}	method	ref
Ca^{2+}	0.28	2.47	3.1	9.2	classical MD	this work
	0.28	2.38	2.9	10	QM/MM MD (STO−3G)	this work
	0.28	2.45	3.3	8.3	QM/MM MD (LANL2DZ)	this work
	0.16	2.5		8.6	PCM MD	20
	0.26	2.5	3.5	8	classical MD	6
	0.45	2.5		7.9	classical MD	7
$CaCl_2$	1.1	2.39	3.2−3.7	9.2	classical MD	4
$CaCl_2$	1.0	2.42		6	XD	10
	2.0	2.41		6	XD	10
	4.5	2.42		6	XD	10
	1.1	2.39		6.9	XD	4
	6.5	2.44		6	XD	11
	4.5	2.40		5.5	ND	8
	1.0	2.46		10	ND	9
	2.8	2.39		7.2	ND	9
	4.5	2.41		6.4	ND	9

this work, this recently proposed scheme will be used to study the solution of Ca^{2+} in water. In sections 2 and 3, the method will be briefly described and the details of the simulations will be given.

2. Method

The system is partitioned into a part described quantum mechanically and another part treated by means of molecular mechanics. The interactions within the "quantum mechanical (QM) region" are evaluated on the basis of ab initio Born−Oppenheimer (BO) dynamics,[28] whereas those interactions within the "molecular mechanical (MM)" and between "quantum mechanical" and "molecular mechanical" regions are calculated using classical pair potentials.

The quantum mechanical forces inside the QM region can be obtained from analytic gradients[37] as the pair potential forces can be derived analytically from the pair potential functions. The force on one particle in the system is defined as

$$F_i = S_m(r)F_{QM} + (1 - S_m(r))F_{PP} \qquad (2)$$

where F_{QM} and F_{PP} are forces from quantum mechanics and pair potentials, respectively. r is the distance between the calcium ion and the center of mass of water. $S_m(r)$ is a smoothing function[38] applied to ensure a continuous change of forces at the transition between QM and MM region,

$$S_m(r) = 1 \qquad \text{for } r \le r_1$$

$$S_m(r) = \frac{(r_0^2 - r^2)^2(r_0^2 + 2r^2 - 3r_1^2)}{(r_0^2 - r_1^2)^3} \qquad r_1 < r \le r_0$$

$$S_m(r) = 0 \qquad \text{for } r > r_0$$

where r_1 and r_0 are the ion−water distances characterizing the start and finish of the shell, where smoothing applies.

3. Calculations

Three molecular dynamics simulations were carried out:

(1) Traditional molecular dynamics simulation using classical pair potentials.

(2) Combined QM/MM molecular dynamics simulation performed at Hartree−Fock level using STO-3G basis sets[39,40] for all atoms.

(3) Combined QM/MM molecular dynamics simulation performed at Hartree−Fock level using full double-ζ (DZ) basis set[41] for H_2O and Los Alamos ECP plus DZ basis set[42] for Ca^{2+} (corresponding to the LANL2DZ basis set keyword in Gaussian 94 series of programs[43]).

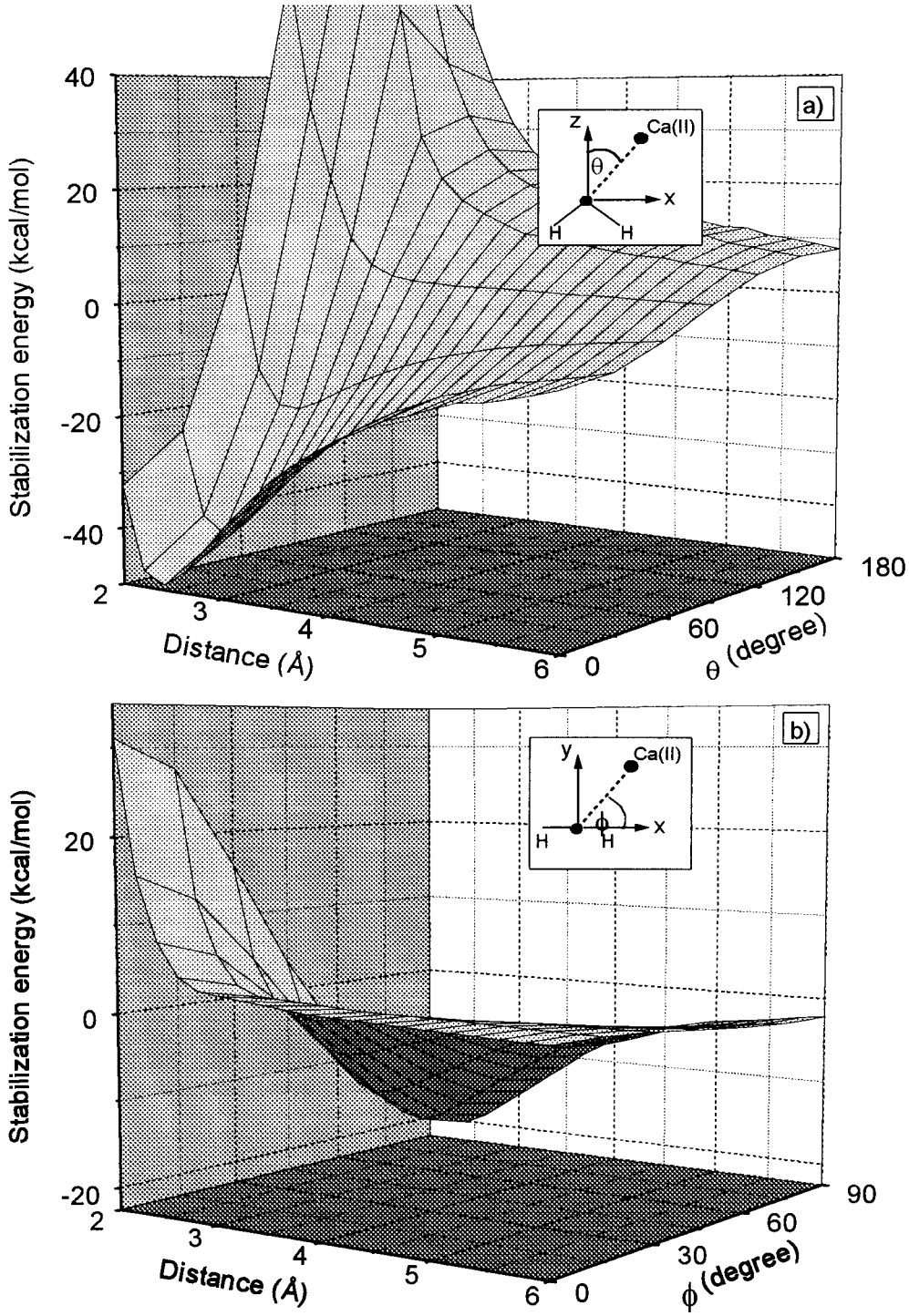

Figure 2. Selected parts of the potential energy surface of the fitted function with respect to some movements of calcium ion around water molecule. (a) ϕ is fixed at 0 degrees and θ varied; (b) θ is fixed at 90° and ϕ varied.

The pair potential function for $Ca^{2+}-H_2O$ was newly constructed. 1800 Hartree−Fock interaction energy points, using the DZV+(d,p) basis set[41] for H_2O and Los Alamos ECP plus DZ basis set[42] for Ca^{2+}, were fitted to an analytical form:

$$\Delta E_{FIT} = \sum_{i=1}^{3} \frac{A_{ic}}{r_{ic}^{6}} + \frac{B_{ic}}{r_{ic}^{7}} + C_{ic} \exp(-D_{ic} r_{ic}) + \frac{q_i q_c}{r_{ic}} \quad (4)$$

where A, B, C and D are the fitting parameters (see Table 1) and r denotes the distances between calcium ion and atoms of water. The subscripts i and c indicate the ith atom of a water molecule and calcium ion, and q are atomic charges. The charge on Ca was assumed to be 2.0 and that on O and H of water[44] −0.6598 and 0.3299, respectively. All ab initio calculations were done using the Gaussian 94 series of programs.[43]

The quality of the fit is shown in Figure 1 where the stabilization energies obtained from the SCF calculations (ΔE_{SCF}) and from the fitted potential function (ΔE_{FIT}) are compared for some orientations. Parts of the potential energy surface of the fitted function are also shown in Figure 2a,b, representing some movements of calcium ion around the water molecule. The function exhibits a stabilization energy of −49.6 kcal mol^{-1} at a $Ca^{2+}-O$ distance of 2.37 Å with the calcium ion placed in the optimal position for interaction with the dipole moment of water.

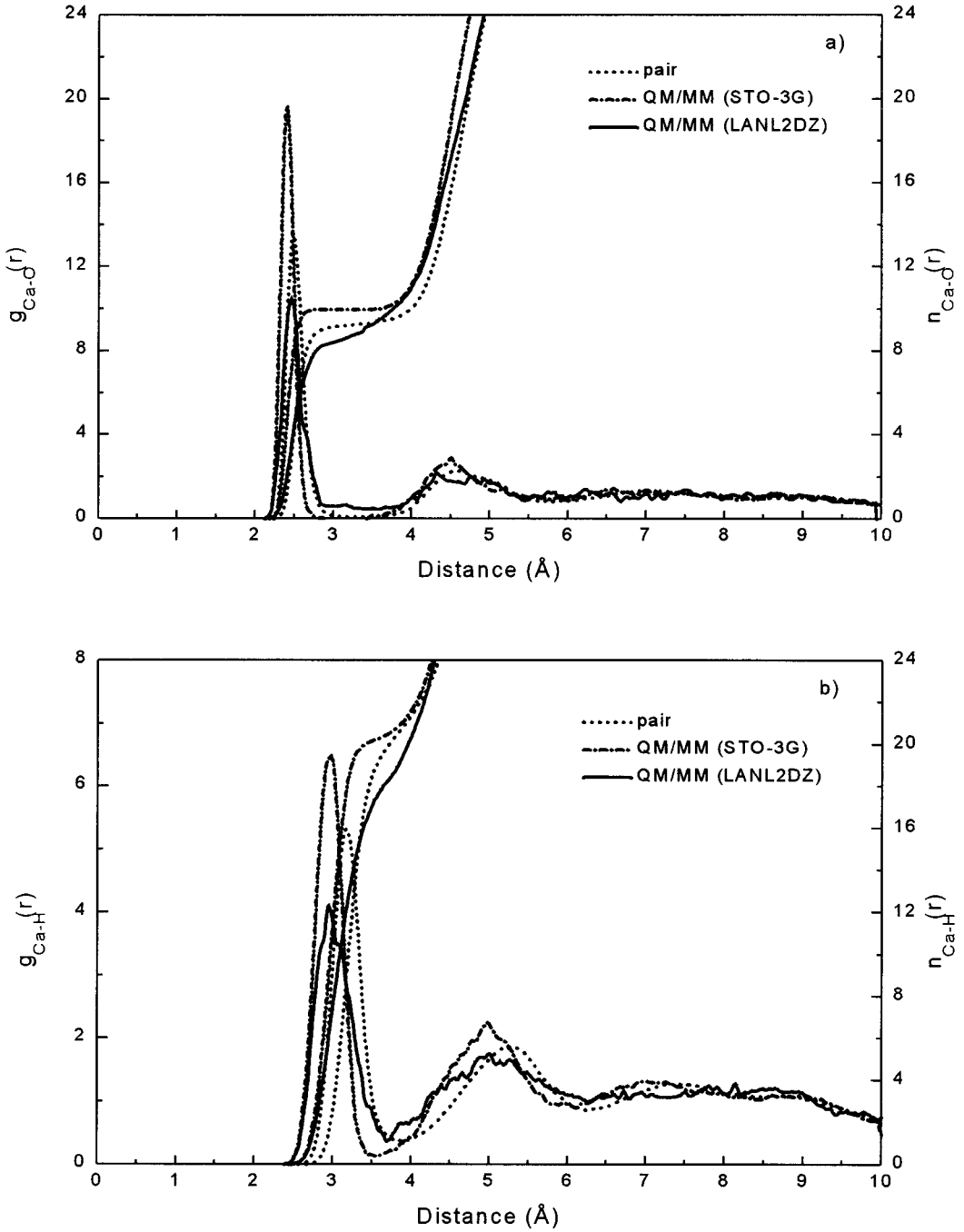

Figure 3. (a) Ca−O and (b) Ca−H radial distribution functions and their corresponding integration numbers.

The simulation using pair potentials only was performed first. The combined QM/MM molecular dynamics simulations using STO-3G basis set and LANL2DZ basis set were investigated subsequently, using the equilibrium configuration obtained from this "traditional" simulation. The reaction-field procedure[45] was employed in all simulations to correct the cutoff of long-range interactions. Since the computational effort (i.e., CPU time) for ab initio forces calculation is considerable, the size of the QM region should not be chosen too large. Therefore, the diameter of the first solvation shell of Ca^{2+} obtained from the traditional pair potential simulations was used to define the size of this region. An interval of 0.2 Å was applied for the smoothing function (i.e., in eq 3, $r_0 = 3.6$ Å and $r_1 = 3.4$ Å). All simulations were carried out in a canonical ensemble consisting of one Ca^{2+} and 199 water molecules at 298 K using a box of 18.19 Å length, corresponding to the density of pure water. A flexible model for water including intermolecular[44] and intramolecular potentials[46] was employed, and a time step of 0.2 fs was chosen. The "classical" molecular dynamics simulation started from a random configuration and was equilibrated for 20 000 time steps. The simulation was continued for 60 000 time steps to collect configurations every 10th step. The combined QM/MM molecular dynamics simulation using STO-3G basis set was reequilibrated for 15 000 time steps and another 20 000 time steps were subsequently performed to collect configurations every fifth step. The last QM/MM molecular dynamics simulation using LANL2DZ basis sets was reequilibrated for 10 000 time steps and the following 8000 time steps were used to collect configurations every fourth step.

4. Results and Discussion

4.1. Structural Properties. *4.1.1. Solvation Shell Structure of Calcium Ion in Water.* The Ca−O and Ca−H radial distribution functions for all three molecular dynamics simulations are shown in Figure 3a,b, respectively. The solvation

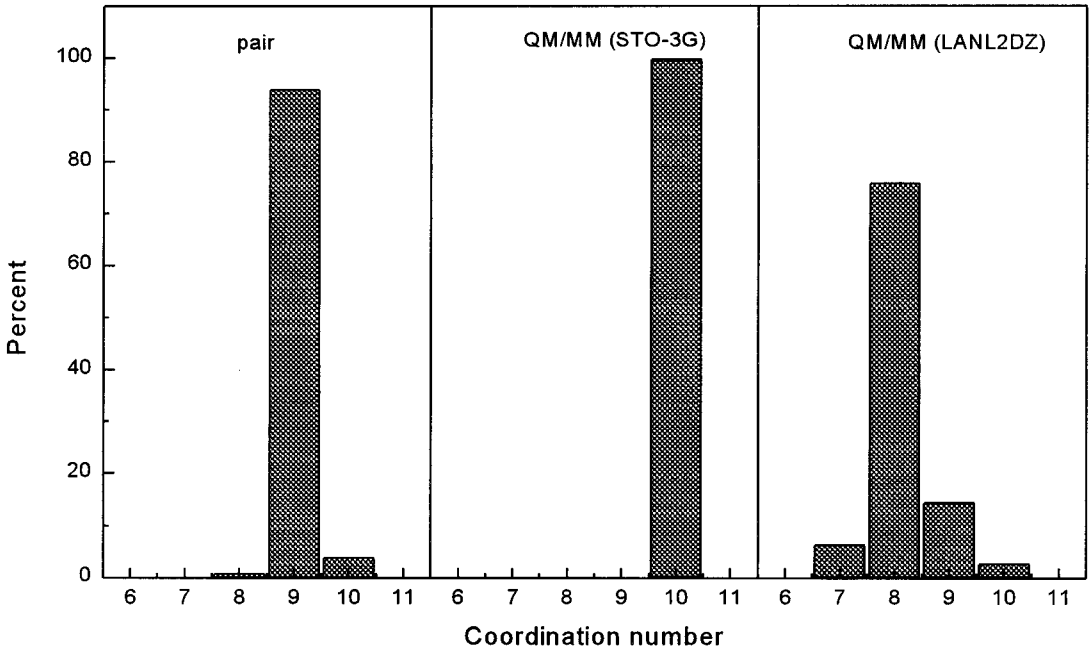

Figure 4. Probability of coordination number distributions.

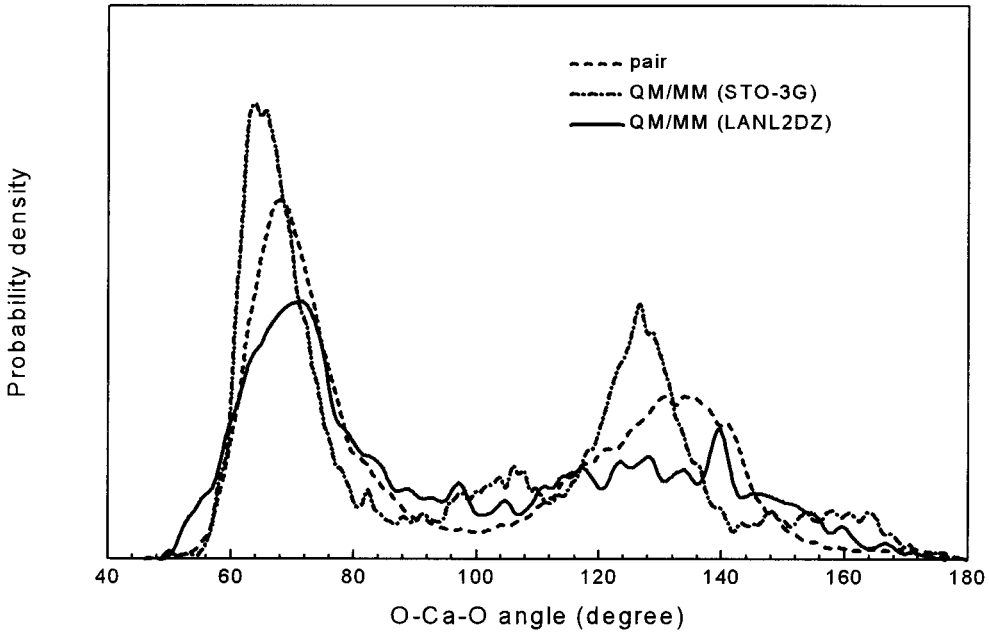

Figure 5. O−Ca−O angular distribution up to the first minimum of the Ca−O RDFs.

parameters are compared with other theoretical simulations and experimental investigations in Table 2. The first Ca−O maximum obtained from classical pair potential molecular dynamics simulation is centered at 2.47 Å, and the first solvation shell is well separated from the second one, giving the average coordination number of 9.2. These characteristic values are in agreement with another classical molecular dynamics simulation of 1.1 M $CaCl_2$ aqueous solution.[4] The Ca−O peak of the QM/MM (STO-3G) simulation exhibits the first maximum at 2.38 Å. Also in this simulation the first solvation shell is clearly separated and yields a coordination number of 10. This increase can be explained by the use of this small basis set, which generally give overestimated interaction energies and hence shorter ion−O distances, and therefore also a higher coordination number. With improved quality of the basis set, as seen in the QM/MM (LANL2DZ) simulation, the first maximum Ca−O peak is found at 2.45 Å. The RDF then shows a broad minimum, ranging from 2.9 to 3.8 Å, and leads to an average coordination number of 8.3 for the first shell. Figure 4 shows the probability distributions of the coordination numbers, calculated up to a Ca−O distance of 3.0 Å. A preferred coordination number of 9 is found for the simulation with the classical pair potential, 10 for the combined QM/MM (STO-3G) and 8 for the combined QM/MM (LANL2DZ) simulation, respectively.

One might doubt that the change in the coordination numbers could be influenced by different equilibrium angles of water within the different methods. The MM water presumably has a bond angle close to experimental value of 104.5°, whereas the optimized water angles with STO-3G and LANL2DZ basis sets yield by about 100 and 112°, respectively. To analyze this point, a pair potential simulation in which the equilibrium angle of water was changed within the intramolecular water potential to 112° was performed. We found only a very small decrease in the average coordination number from 9.2 to 9.0. Therefore, it is obvious that the different angles for the water equilibrium

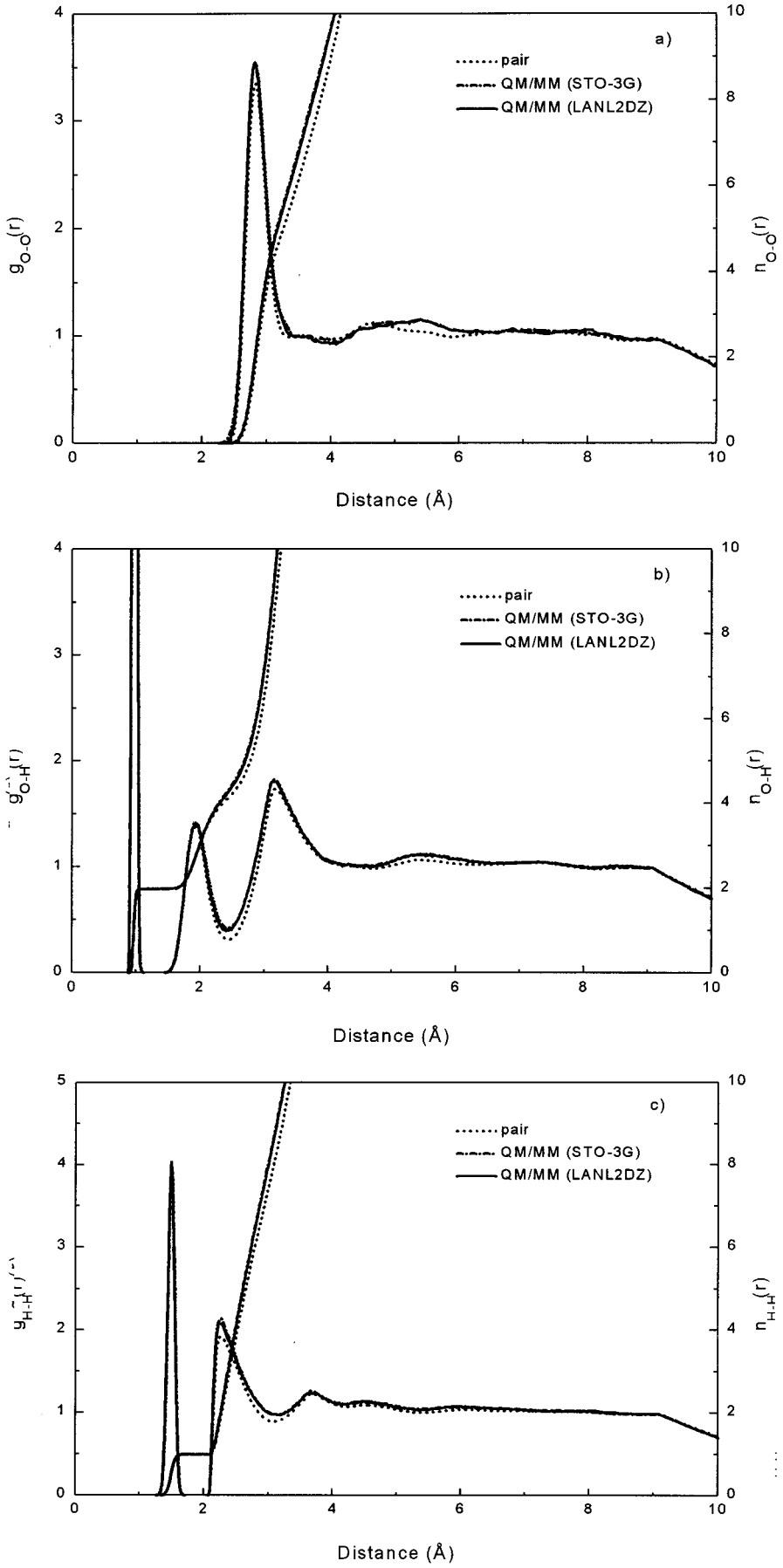

Figure 6. (a) O−O, (b) O−H, and (c) H−H radial distribution functions and their corresponding integration numbers.

structure cannot explain the observed change in the average coordination number.

The most reliable coordination number distribution obtained from the QM/MM (LANL2DZ) simulation illustrates clearly that $Ca(H_2O)_8^{2+}$ is by no means the exclusive species represented in the solution. Ions coordinated to 9, 7, and 10 water

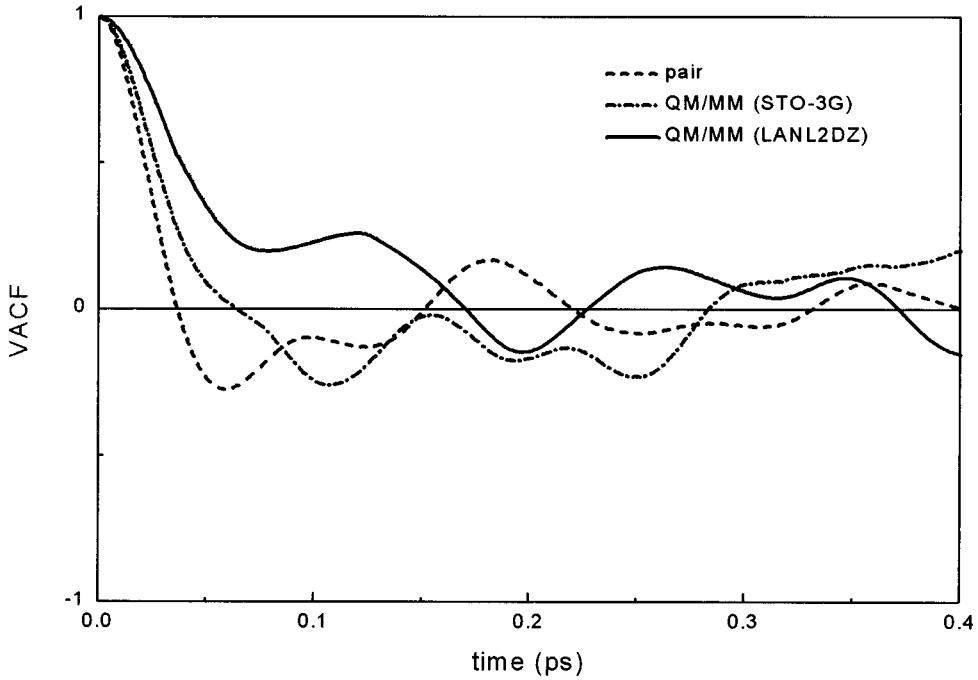

Figure 7. Velocity autocorrelation functions of Ca^{2+}.

molecules (in decreasing amount) coexist with this main species. This rather complex situation helps to understand difficulties in setting up suitable models fitting X-ray or neutron diffraction patterns. At higher concentration and in the presence of counterions, this variability of solvate species should become even more complex in analogy to similar salt solutions.[47,48]

Figure 5 displays the O−Ca−O angular distributions up to the first minimum of the Ca−O RDFs. The approximate solvation shell structure for coordination numbers 9 and 10 are polyhedrals belonging to D_{3h} and D_{4d} point groups, respectively, as discussed by Pálinkás and Heinzinger.[49] For the coordination number of 8, there are three possible structures: dodecahedron, cube and square antiprism. The cube structure can be excluded due to the fact that in the O−Ca−O angular distribution at neither 90° nor 180° considerable probability density is found. Therefore, the structure of the Ca^{2+} with the coordination number of 8.3 obtained from the QM/MM (LANL2DZ) simulation can be expected to be either a dodecahedron or a square antiprism. Other simulations based on classical pair potential[6] and using ab initio effective pair potential based on PCM[20] also gave similar coordination numbers of 8, an antiprism with C_{4v} symmetry, and 8.6, respectively. The authors suggested that their values seemed too low compared to literature data[6] and also assumed that nonadditive effects would not reduce the Ca^{2+}−water binding energy substantially.[20] We believe that our results finally prove that the lower coordination number of 8 is realistic and that early experiments[9] yielding very high coordination numbers should be seen with much caution.

4.1.2. Solvent Structure. The O−O, O−H, and H−H radial distribution functions and their corresponding integration numbers are shown in Figure 6a−c, respectively. Since the combined QM/MM method performs quantum mechanical calculations just in the first solvation shell of Ca^{2+}, i.e., about less than 5% of the overall volume of the system, the properties of the solvent structure obtained from the classical pair potential and combined QM/MM simulations are both expected to be equivalent within the statistical fluctuation. In fact, their characteristic values obtained from classical pair potentials do not show significant differences when compared with other classical pair potential simulations[4,50] of $MgCl_2$ or $CaCl_2$ in aqueous solution.

4.1.3. Intramolecular Geometry of Solvent Molecules. The use of a flexible model for water allows the investigation of the influence of the ion on the intramolecular geometry of solvent molecules. The effect of the ion observed from the classical pair potential, the QM/MM (STO-3G) and the QM/MM (LANL2DZ) simulations is a shift of the O−H bond length toward longer distances. In addition, a smaller H−O−H angle is found in all three cases. The decrease of the coordination number from 9.2 to 8.3 from the classical pair potential simulation to the QM/MM (LANL2DZ) simulation reduces this effect, due to the decrease of H−H repulsion between neighboring water molecules in the solvation shell of Ca^{2+}.

4.2. Dynamical Properties. *4.2.1. Hindered Translational Motion.* Due to the relatively short time of the combined QM/MM simulations, the dynamical properties have to be considered with special care and should not be overinterpreted. An overview of the particle motions can be gained by computing the velocity autocorrelation functions (VACFs). The VACFs for Ca^{2+} are depicted in Figure 7. The combined QM/MM simulations cause the VACFs to decay slower than in the classical pair potential simulation, indicating that the many-body effects allow a more free translational motion of Ca^{2+} in the solution. For water, the hindered translations are studied by the center-of-mass VACFs of the water molecules. The VACFs and their Fourier transformations were determined separately for water in the bulk and in the solvation shell. The VACFs are shown in Figure 8 and their Fourier transforms in Figure 9. The bulk VACFs exhibit a maximum at about 60 cm^{-1} and a broad band around 200 cm^{-1}. These two pronounced peaks are identified as hindered translational motions of the center-of-mass parallel and perpendicular to the dipole vector of water molecules which have been attributed to the hydrogen bond bending and the O−O stretching motions, respectively.[51] In the presence of Ca^{2+}, the peaks in the spectra obtained from all three molecular dynamics simulations are shifted to higher frequencies, for both the parallel and perpendicular motions, due to the strong binding between ion and water as well as because of the increase of the mutual interaction between the water molecules compressed in the solvation sphere by the strong electric field of the ion. The QM/MM (STO-3G) simulation exhibits the highest peak at about 290 cm^{-1} as

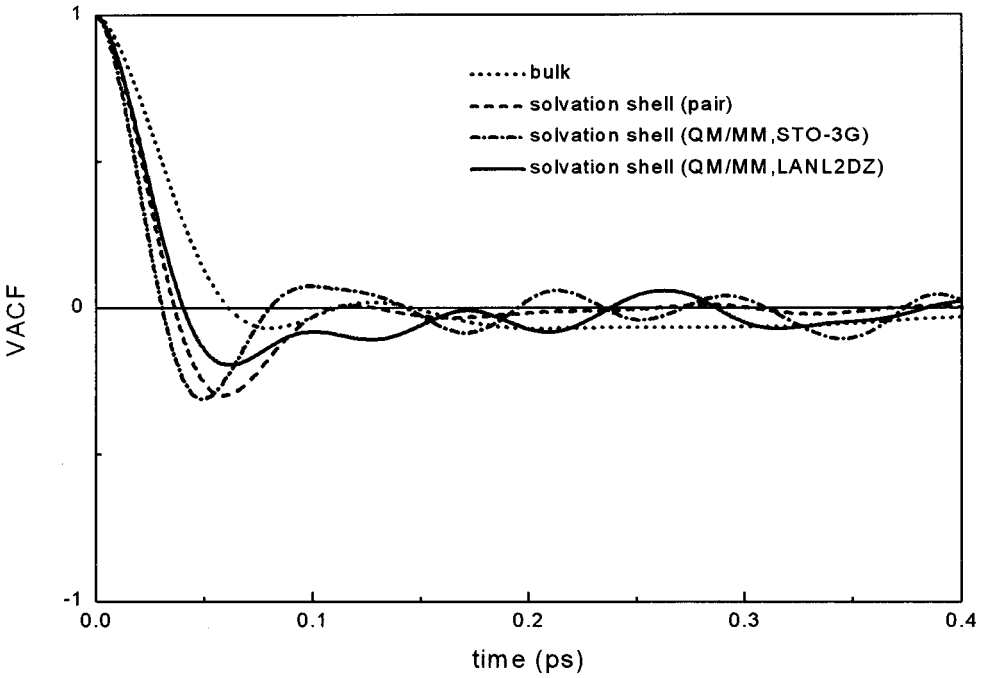

Figure 8. Velocity autocorrelation functions of the center of mass of water.

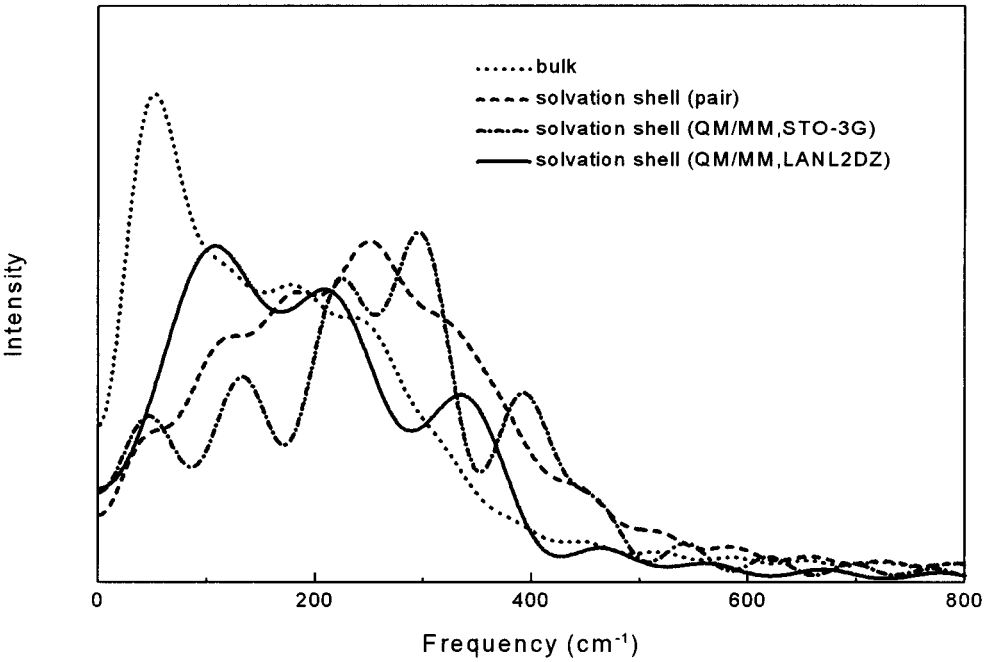

Figure 9. Fourier transforms of the translational motions of water, calculated from the center of mass VACFs of water.

expected from the use of a small basis set that overestimates the binding energy between ion and water in the solvation shell. In contrast to that, the other QM/MM (LANL2DZ) simulation shows a much smaller influence of Ca^{2+} on the translational motion of water molecules in the solvation shell by giving the maximum peak at around 115 cm^{-1}. This illustrates that the inclusion of many-body effects by using a QM/MM method with a reasonable basis set results in weaker Ca^{2+}−water interactions and therefore in a lower frequency shift.

4.2.2. Librational Motion. The VACFs and their corresponding Fourier transformations for the librational motions are shown in Figures10 and 11. The three axes, η, ξ, and ζ, were chosen as identical with the three principal moments of inertia employed in the description of the rotations of the rigid molecule.[52] The VACFs around the approximated η axis decay faster than the motions around the approximated ξ and ζ axis, and hence they give peaks at the highest frequencies. As can be seen in Figure 11, in the solvation shell of Ca^{2+}, the influence of the ion shifts the peaks to higher frequencies due to the strong interactions between ion and water. The peaks obtained both from the QM/MM (STO-3G) and the QM/MM (LANL2DZ) simulation lead to rather large shifts to higher frequencies. As mentioned above, the use of the small basis set in the QM/MM (STO-3G) results in too strong Ca^{2+}−water interactions and hence gives the shortest Ca−O distance and the highest coordination number. This increase of the steric hindrance in the solvation shell leads to high-frequency shifts. For the QM/MM (LANL2DZ) simulation, the shift to higher frequencies can be understood from the intramolecular geometry of water molecules inside the solvation shell. The wider H−O−H angle also results in an increase of steric hindrance and therefore also in a shift to higher frequencies.

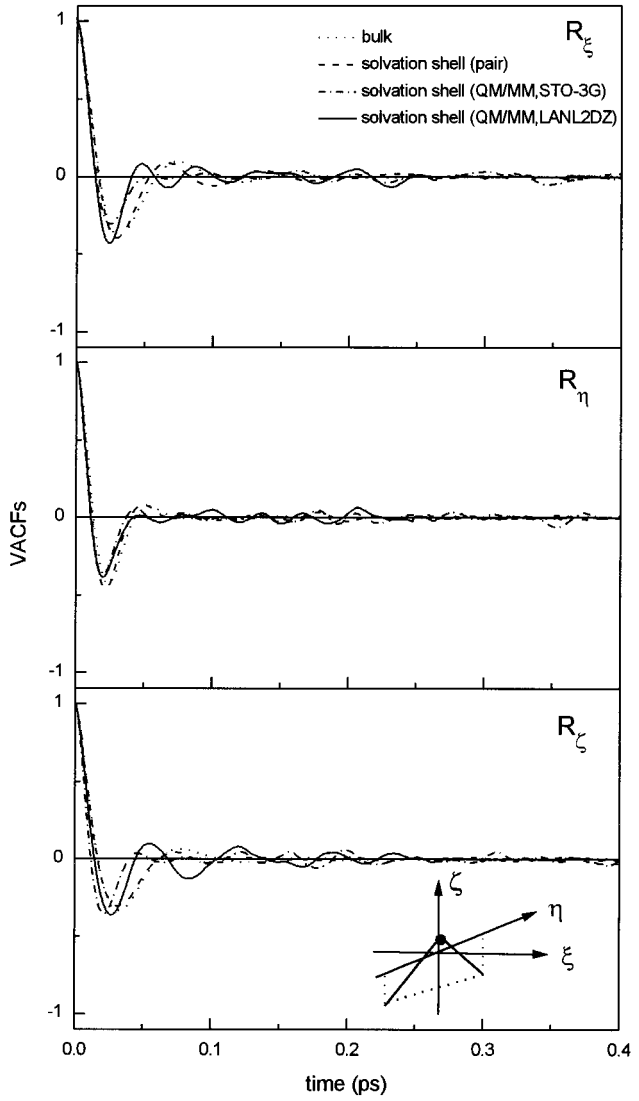

Figure 10. Velocity autocorrelation functions of water around the approximated ξ, η, and ζ axes.

4.2.3. Vibrational Motion. Fourier transforms of VACFs for obtaining infrared spectra are usually discussed only in terms of shifts of peak maxima as a result of the ionic influence. The frequencies are calculated from the VACFs of hydrogens using a normal-coordinate analysis developed by Bopp.[53] The three quantities Q_1, Q_2, and Q_3 are defined for describing each water molecule in terms of symmetric stretching and bending and asymmetric stretching motions, respectively. For the classical pair potential simulation, the vibrational motions are dominated by an analytical intramolecular potential which is fitted separately from the intermolecular potential to reproduce the experimental intramolecular motions. In contrast to this procedure, there is no separation between inter- and intramolecular interaction in the combined QM/MM method. The vibrational motions are governed by the Newtonian equation of motion characterized by ab initio forces. For reasons of comparison, the vibrational frequencies for water in the gas phase were also calculated at the Hartree−Fock level using the same basis sets employed in the combined QM/MM simulations. Due to rather constant systematic errors of Hartree−Fock frequencies a scaling factor of 0.89 was proposed to scale the computed frequencies to be in agreement with the experiment.[54−56] Therefore all ab initio results in this work were scaled with this proposed factor. The bending and stretching frequencies are shown in Figure 12a−d, calculated separately for water in the bulk and in the solvation shell of Ca^{2+}. An overview of the intramolecular

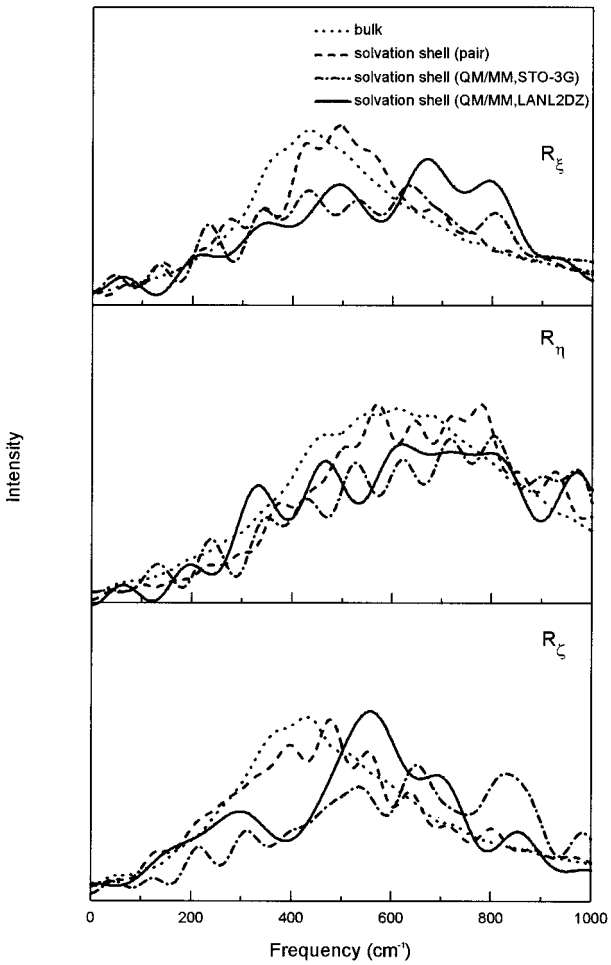

Figure 11. Fourier transforms of the librational motions of water, calculated from the VACFs of water around the approximated ξ, η, and ζ axes.

vibrational frequencies of water obtained from various simulations and experiments is given in Table 3. In the bulk, a peak maximum at 1710 ± 4 cm^{-1} was found for the symmetric bending and peak maxima at 3497 ± 8 and 3644 ± 3 cm^{-1} were found for symmetric and asymmetric stretching, respectively. In the solvation shell of Ca^{2+}, the bending and stretching frequencies have a blue-shift for the QM/MM (STO-3G) simulation but a red-shift for the classical pair potential simulation and the QM/MM (LANL2DZ) simulation. The blue-shift for both bending and stretching modes in the QM/MM (STO-3G) simulation are simply due to the inadequate small basis set and will not be discussed further. In comparison with the classical pair potential simulation, the frequencies obtained from the QM/MM (LANL2DZ) simulation show a smaller red-shift for the stretching vibration but a larger red-shift for the bending vibration. The red-shift in the stretching frequencies reflects the Ca−O attraction and Ca−H repulsion that elongate the O−H bond length. The inclusion of many-body terms in the QM/MM (LANL2DZ) simulation results in a smaller influence of Ca^{2+} on the Ca^{2+}−water interactions, leading to smaller changes of the O−H bond length. The shift of the bending frequency can be understood in terms of the H−H repulsion between the water molecules. In the QM/MM (LANL2DZ) simulation, this effect is less pronounced than in the pair potential simulation due to the weaker Ca^{2+}−water interactions and smaller average coordination number which causes wider H−O−H angles.

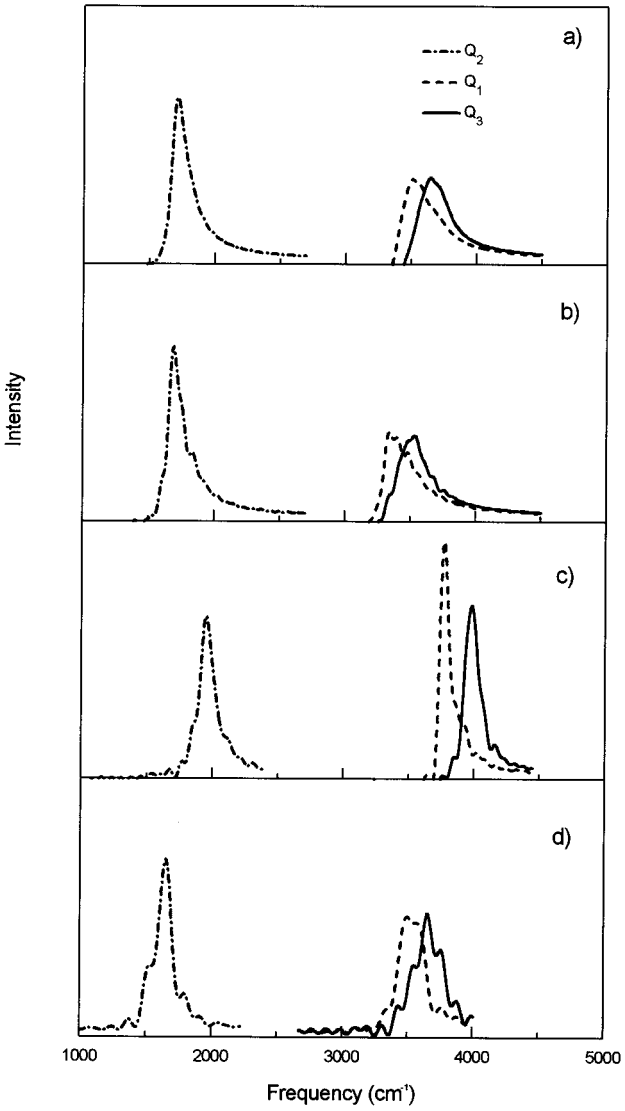

Figure 12. Fourier transforms of the hydrogen velocity autocorrelation functions: (a) bulk water, (b) solvation shell of Ca^{2+} (classical pair potential), (c) solvation shell of Ca^{2+} (QM/MM (STO-3G)), and (d) solvation shell of Ca^{2+} (QM/MM (LANL2DZ)).

5. Conclusion

The combined QM/MM molecular dynamics simulations which include the major part of the many-body contributions—by definition all in the first solvation shell of Ca^{2+}—have shown the significant role of the many-body interactions not only for the structural but also for the dynamical properties of the solution. The choice of basis sets in this method is obviously a most crucial parameter for the validity of the conclusions. The LANL2DZ basis set seems to offer a good compromise between the enormous computational demands and the desired accuracy. This seem of special importance, as many of the nowadays used pair and three-body potentials for ion−solvent interactions have been developed with comparable basis sets.

We consider our results as a proof for the increasing tendency to assume a lower coordination number of solvated Ca^{2+}, in contrast to many earlier studies. The results also demonstrate that classical pair and sometimes even three-body simulations can give a somewhat misleading picture of the solvation of charged ions, because they are principally not capable of reproducing the complex electronic effects occurring in the first solvation shell of a double-charged ion.

TABLE 3: Comparison of the Intramolecular Vibrational Frequencies of Water Obtained from Various Simulations and Experiments (Q_1, Q_2, and Q_3 Corresponding to Symmetric Stretching, Bending, and Asymmetric Stretching Vibrations, Respectively)

	frequency (cm^{-1})			
phase	Q_1	Q_3	Q_2	ref
bulk	3506	3647	1714	this work, pair potential
	3480	3641	1712	this work, QM/MM (STO−3G)
	3489	3643	1706	this work, QM/MM (LANL2DZ)
	3475	3580	1715	53
	3527		1715	57
	3345[d]	3445[d]	1645[d]	60
solvation	3339	3536	1688	this work, pair potential
shell	3769	3981	1949	this work, QM/MM (STO−3G)
	3465	3636	1650	this work, QM/MM (LANL2DZ)
	3160	3285	1685	53
	3208		1689	57
gas	3683[a]	3907[a]	1931[a]	this work (STO−3G)
	3584[a]	3741[a]	1660[a]	this work (LANL2DZ)
	3832[b]	3943[b]	1649[b]	58
	3657[c]	3756[c]	1595[c]	59

[a] Computed frequencies in the gas phase (scaled). [b] Simulation frequencies in the gas phase. [c] Experimental frequencies in gas phase. [d] Experimental frequencies in liquid water.

Acknowledgment. We are grateful for financial support by the Forschungsförderungsfonds of Austria (Project P11683-PHY).

References and Notes

(1) Clapham, D. E. *Cell* **1995**, *80*, 259.
(2) Chazin, W. J. *Nat. Struct. Biol.* **1995**, *2*, 707.
(3) Bounds, D. G. *Mol. Phys.* **1985**, *54*, 1335.
(4) Probst, M. M.; Radnai, T.; Heinzinger, K.; Bopp, P.; Rode, B. M. *J. Phys. Chem.* **1985**, *89*, 753.
(5) Pálinkás, G.; Heinzinger, K. *Chem. Phys. Lett.* **1986**, *126*, 251.
(6) Obst, S.; Bradaczek, H. *J. Phys. Chem.* **1996**, *100*, 15677.
(7) Kalko, S. G.; Sesé, G.; Padró, J. A. *J. Chem. Phys.* **1996**, *104*, 9578.
(8) Cummings, S.; Enderby, J. E.; Howe, R. A. *J. Phys. C* **1980**, *13*, 1.
(9) Hewish, N. A.; Neilson, G. W.; Enderby, J. E. *Nature* **1982**, *297*, 138.
(10) Licheri, G.; Piccaluga, G.; Pinna, G. *J. Chem. Phys.* **1976**, *64*, 2437.
(11) Yamaguchi, T.; Hayashi, S.; Ohtaki, H. *Inorg. Chem.* **1989**, *28*, 2434.
(12) Neilson, G. W.; Enderby, J. E. *Adv. Inorg. Chem.* **1989,** *34*, 195.
(13) Katz, A. K.; Glusker, J. P.; Beebe, S. A.; Bock, C. W. *J. Am. Chem. Soc.* **1996**, *118*, 5752.
(14) Beaumont, R. H.; Chihara, H.; Morrison, J. A. *Proc. Phys. Soc.* **1961**, *78*, 1462.
(15) Ermakova, E.; Solca, J.; Huber H.; Marx, D. *Chem. Phys. Lett.* **1995**, *246*, 204.
(16) Probst, M. M.; Spohr, E.; Heinzinger, K.; Bopp, P. *Mol. Simul.* **1991**, *7*, 43.
(17) Ortega-Blake, I.; Novaro, O.; Lés, A.; Rybak, S. *J. Chem. Phys.* **1982**, *76*, 5405.
(18) Lybrand, T. P.; Kollman, P. A. *J. Chem. Phys.* **1985**, *83*, 2923.
(19) Miertus, S.; Scrocco, E.; Tomasi, J. *Chem. Phys.* **1981**, *55*, 117.
(20) Floris, F. M.; Persico, M.; Tani, A.; Tomasi, J. *Chem. Phys. Lett.* **1994**, *227*, 126.
(21) Berendsen, H. J. C.; Grigera, J. R.; Straatsma, T. P. *J. Phys. Chem.* **1987**, *91*, 6269.
(22) Hermansson, K.; Lindgren, J.; Probst, M. M. *Chem. Phys. Lett.* **1995**, *233*, 371.
(23) Perakis, I. E. *Chem. Phys.* **1996**, *210*, 259.
(24) Car, R.; Parrinello, M. *Phys. Rev. Lett.* **1985**, *55*, 2471.
(25) Kirkpatrick, S.; Gelatt Jr., C. D.; Vecchi, M. P. *Science.* **1983**, *220*, 671.
(26) Tsoo, C.; Estrin, D. A.; Singer S. J. *J. Chem. Phys.* **1990**, *93*, 7187.
(27) Andreoni, W.; Gygi, F.; Parrinello, M. *Chem. Phys. Lett.* **1992**, *189*, 241.
(28) Warshel, A.; Karplus, M. *J. Am. Chem. Soc.* **1972**, *94*, 5612.
(29) Allinger, N. L.; Sprague, J. T. *J. Am. Chem. Soc.* **1973**, *95*, 3893.
(30) Dunning Jr., T. H.; Harding, L. B.; Wagner, A. F.; Schatz, G. C.; Bowman, J. M. *Science* **1988**, *240*, 453.

(31) Bauschlicher, C. W.; Walch, S. P.; Langhoff, S. R.; Taylor, P. R.; Jaffe, R. L. *J. Chem. Phys.* **1988**, *88*, 1743.
(32) Bash, P. A.; Field, M. J.; Karplus, M. *J. Am. Chem. Soc.* **1987**, *109*, 8092.
(33) Gao, J. *J. Am. Chem. Soc.* **1993**, *115*, 2930.
(34) Liu, H.; Müller-Plathe, F.; van Gunsteren, W. F. *J. Chem. Phys.* **1995**, *102*, 1722.
(35) Field, M. J.; Bash, P. A.; Karplus, M. *J. Comput. Chem.* **1990**, *11*, 700.
(36) Kerdcharoen, T.; Liedl, K. R.; Rode, B. M. *Chem. Phys.* **1996**, *211*, 313.
(37) Pulay, P. *Ab initio methods in quantum chemistry II*; Lawley, K. P., Ed.; Wiley: New York, 1987; p 241.
(38) Brooks, B. R.; Bruccoleri, R. E.; Olafson, B. D.; States, D. J.; Swaminathan, S.; Karplus, M. *J. Comput. Chem.* **1983**, *4*, 187.
(39) Hehre, W. J.; Stewart, R. F.; Pople, J. A. *J. Chem. Phys.* **1969**, *51*, 2657.
(40) Collins, J. B.; Schleyer, P. v. R.; Binkley, J. S.; Pople, J. A. *J. Chem. Phys.* **1976**, *64*, 5142.
(41) Dunning Jr., T. H.; Hay, P. J. *Modern theoretical chemistry*; Plenum: New York, 1976; p 1.
(42) Wadt, W. R.; Hay, P. J. *J. Chem. Phys.* **1985**, *82*, 284.
(43) Frisch, M. J.; Trucks, G. W.; Schlegel, H. B.; Gill, P. M. W.; Johnson, B. G.; Robb, M. A.; Cheeseman, J. R.; Keith, T. A.; Peterson, G. A.; Montgomery, J. A.; Raghavachari, K.; Al-Laham, M. A.; Zakrzewski, V. G.; Ortiz, J. V.; Foresman, J. B.; Cioslowski, J.; Stafanov, B. B.; Nanayakkara, A.; Challacombe, M.; Peng, C. Y.; Ayala, P. Y.; Chen, W.; Wong, M. W.; Andres, J. L.; Replogle, E. S.; Gomperts, R.; Martin, R. L.; Fox, D. J.; Binkley, J. S.; Defrees, D. J.; Baker, J.; Stewart, J. P.; Head-Gordon, M.; Gonzalez, C.; Pople, J. A. *GAUSSIAN 94;* Gaussian, Inc.: Pittsburgh, PA, 1995.
(44) Stillinger, F. H.; Rahman, A. *J. Chem. Phys.* **1978**, *68*, 666.
(45) Adams, D. J.; Adams, E. H.; Hills, G. J. *Mol. Phys.* **1979**, *38*, 387.
(46) Bopp, P.; Jancsó, G.; Heinzinger, K. *Chem. Phys. Lett.* **1983**, *98*, 129.
(47) Texler, N. R.; Rode, B. M. *J. Phys. Chem.* **1995**, *99*, 15714.
(48) Rode, B. M. *J. Phys. Chem.* **1992**, *96*, 4170.
(49) Pálinkás, G.; Heinzinger, K. *Chem. Phys. Lett.* **1986**, *126*, 251.
(50) Dietz, W.; Riede, W. O.; Heinzinger, K. *Z. Naturforsch.* **1982**, *37a*, 1038.
(51) Sceats, M. G.; Rice, S. A. *J. Chem. Phys.* **1980**, *72*, 3236.
(52) Szász, Gy. I.; Heinzinger, K. *J. Chem. Phys.* **1983**, *79*, 3467.
(53) Bopp, P. *Chem. Phys.* **1986**, *106*, 205.
(54) Pople, J. A.; Krishnan, R.; Schlegel, H. B.; DeFrees, D. J.; Binkley, J. S.; Frisch, M. J.; Whiteside, R. A.; Hout, R. F.; Hehre, W. J. *Int. J. Quantum Chem. Symp. 15* **1981**, 269.
(55) DeFrees, D. J.; McLean, A. D. *J. Chem. Phys.* **1985**, *82*, 333.
(56) Grev, R.S.; Janssen, C. L.; Schaefer, H. F., III. *J. Chem. Phys.* **1991**, *95*, 5128.
(57) Probst, M. M.; Bopp, P.; Heinzinger, K.; Rode, B. M. *Chem. Phys. Lett.* **1984**, *106*, 317.
(58) Jancsó, G.; Bopp, P. *Z. Naturforsch.* **1983**, *38a*, 206.
(59) Eisenberg, D.; Kauzmann, W. *The structure and properties of water*; Oxford University Press: Oxford, 1969.
(60) Murphy, W. F.; Bernstein, H. J. *J. Phys. Chem.* **1972**, *76*, 1147.